Patterning of Functional Ceramic Oxides on Metallic Substrates by Inkjet Printing

M Vilardell[1,2], X Granados[1], S Ricart[1], A Calleja[1,2], A Palau[1], T Puig[1] and X Obradors[1]
[1] Institut de Ciència dels Materials de Barcelona (ICMAB-CSIC), Campus de la Universitat Autònoma de Barcelona, 08193, Bellaterra, Spain
[2] Oxolutia SL, Edifici Eureka, Parc de Recerca de la UAB, Campus de la UAB, E-08193, Bellaterra, Spain

Abstract

In the search for efficient methodologies focused on up scaling production of low cost functional ceramic oxides, the implementation of Chemical Solution Deposition (CSD) in combination with drop on demand (DoD) inkjet printing technology is a challenge in materials science. When simple additive processing is implemented in continuous reel to reel systems with novel low-cost materials, the potential to further decrease the production costs of the whole manufacturing process is immense.

Sets of parallel $YBa_2Cu_3O_{7-x}$ (YBCO) stripes, 250 nm thick and 150 μm wide, with critical current densities (J_c) of about 1.1 MA/cm^2 at 77K and self field are obtained.

On the other hand, different designs of magnetoresistive $La_{0.7}Sr_{0.3}MnO_3$ (LSMO) devices with electrical resistances in the range of 10 KΩ including the contact pads, are drawn onto $LaAlO_3$ (LAO) and $SrTiO_3$ (STO) single crystals. We particularly investigate different strategies to increase pattern resolution and accuracy. Preliminary morphological and electrical characterizations of the device on cheaper amorphous, polycrystalline and textured substrates are presented.

Therefore, this paper gives a summary of functional ceramic oxides patterning by combining CSD and inkjet printing methodologies onto different single crystal, polycrystalline and textured substrates. The present work demonstrates a powerful method of fabricating multifilamentary YBCO patterned coatings for low losses coated conductors (CC's) and LSMO magnetoresistive analog encoders for position sensing.

Introduction

Functional ceramic oxides are demanded for novel industrial applications in electronics, energy, technology, catalysis, communication, optics and a large etcetera [1-4]. The great potential of these functional ceramic oxides stems from their distinguished functional properties which give added value to existing devices and offers the possibility to explore new fields of interest. However, to fully exploit such innovative areas, increasingly low cost and scalable technologies have to be considered. Moreover, for many applications, it is required to print films and structures of specific shapes and sometimes, even those films are required in an epitaxial quality [5, 6].

In today's processes, the most common techniques for functional ceramic patterning require several steps involving high vacuum, and extremely pure environment [6, 7]. Nevertheless, the exploitation in a large-scale of the well-established physical deposition processing techniques is hampered by their intrinsic technological complexity and low throughput. Additionally, the use of those techniques in device manufacturing usually involves photolithographic post-processing procedures to obtain the final functional pattern [8]. An alternative for this vacuum based technology lies in depositing a metal oxide precursor layer onto a substrate template that after a subsequent thermal treatment gives the desired epitaxial or polycrystalline oxide phase according to the properties of both substrate and ceramic coating. This methodology, overall classified as Chemical Solution Deposition (CSD) [9, 10], in combination with piezoelectric Drop on Demand

(DoD) inkjet printing technology [11], offers interesting benefits such as the possibility to switch conveniently on the flight the pattern design and the coating material providing large versatility to obtain cost-effective high quality devices with specific shapes and dimensions.

In this communication, we present the development of multifilamentary coated conductors (MFCC's) [12] based on (RE)$Ba_2Cu_3O_{7-x}$, ((RE)BCO being RE a rare earth: Y, Sm, Nd and Gd) for ac applications [13]. The present state of the art of low AC losses conductors is based on complex slitting processes very detrimental on material usage (scratching, laser, lithography, etc). In this understanding, inkjet deposition has been demonstrated as a promising election for YBCO patterning to directly obtain multifilamentary structures.

Optimal performances of superconducting coated conductors (CC's) [14] require kilometer length metallic substrates with a previous textured template that provides in-plane and out-of-plane biaxial texture in order to stimulate an epitaxial growth of the superconducting coating. Two methodologies represent the most competitive strategies for the production of textured metallic substrates. The first one is the so called Rolling Assisted Biaxial Texture (RABIT) approach [15], where standard thermo-mechanical processing of the selected metal is utilized to obtain biaxially oriented tape-shaped substrates. The second technique, named Ion Beam Assisted Deposition (IBAD) [16], combines an Ar ion beam with a vacuum based standard ceramic oxide deposition (CVD, PLD and others) to achieve the biaxial texture in the ceramic layer over a non-textured metallic tape. Both metallic substrates have been successfully developed and are commercially available.

On the other hand, within the last years, solution-processable electronics have centered great consideration and research [17]. Inkjet printing of metal precursor inks has been accepted for the manufacturing of microelectronics applications, including conducting wiring for circuitry, radio frequency identification (RFID) tags, organic thin-film transistors (OFET's), organic light

emitting diodes (OLED's), organic photovoltaic disposable displays and sensor arrays.

In the framework of EFECTS (Efficient Environmental-Friendly Electro-Ceramics Coating Technology and Synthesis) project, a fully inkjet-printed $La_{0.7}Sr_{0.3}MnO_3$ (LSMO or manganites as sometimes we will refer herein) contactless magnetoresistive analog encoder has been developed as an example of functional device by combining the low cost and flexible inkjet technology with the CSD methodology. It opens the possibility to incorporate in the same printout both, encoder and circuitry, drastically decreasing so the cost and improving the flexibility for the manufacturing of fully customized production.

Experimental part

For the purposes of YBCO and LSMO patterning, adapted solutions of the corresponding metal-oxides precursors were prepared. Suitable inks require the study of the relevant parameters such as density, surface tension, viscosity, contact angle, and evaporation rate including the different interactions with the substrate and adjusting them to achieve the adequate final pattern.
In this work, we report on two different functional oxides precursor solutions: one for YBCO patterning and the other for LSMO patterning.

Functional oxides precursor solutions

Regarding YBCO patterning, a 0.5M (full metal contents) precursor solution was prepared using the corresponding metal-trifluoroacetates (TFA), ethanol as solvent and 5% w/w 1,3-propanediol for wetting control (see table 1):

Table 1. Rheological and wetting properties of 0.5M ethanol based YBCO precursor solution. All the measurements were performed at room temperature. Viscosity measurement was carried out at a shear rate of 86000 s^{-1}.

	0.5M ethanol based YBCO precursor solution + 5% w/w 1,3-propanediol
Density (g/cm^3)	0.899
Surface tension (mN/m)	22.6
Viscosity (mPa·s)	3.3
Contact angle over LAO single crystal (º)	<10

Further details concerning the preparation methodology of the YBCO precursor solution can be found elsewhere [18]. In the TFA-MOD process and in order to form the YBCO phase, the as-deposited pattern was pyrolyzed at 310 ºC during 30 min to convert the TFA metallic precursors to homogeneous mixtures of nanometric oxide and fluoride phases. A latter growth stage was carried out under a flowing wet gas mixture of oxygen and nitrogen to obtain the tetragonal YBCO phase in a high temperature process (at ~810ºC). Finally, a subsequent oxygenation step at lower temperature was performed to obtain the orthorhombic superconducting phase [9].
The developed LSMO precursor ink for LSMO patterning was based on H_2O, isopropanol and propionic acid in a ratio of 65/34/1 (% in volume). The set of rheological and wetting properties of this solution is listed in table 2:

Table 2. Parameters for the 0.05M (in Mn) water based LSMO precursor solution. All the measurements were performed at room temperature. Viscosity measurement was carried out at a shear rate of 86000 s^{-1}.

	0.05M (in Mn) water based LSMO precursor solution
Density (g/cm^3)	1.020
Surface tension (mN/m)	36.5
Viscosity (mPa·s)	2
Contact angle over LAO and STO single crystals (º)	~40

To obtain the desired LSMO phase, the samples were annealed under air as follows: until 900 ºC with a ramp-up rate of 5 ºC/min, 1h at 900 ºC and a ramp-down rate of 5 ºC/min until room temperature.

Printing

Inkjet deposition was carried out using a commercial piezoelectric actuated dispenser with a 60 µm nozzle diameter mounted in a proprietary mechanical system.

Deposition was performed throughout this work onto $LaAlO_3$ (LAO) and $SrTiO_3$ (STO) single crystals and polycrystalline alumina, fused silica and metallic substrates. Before deposition, single crystals were ultrasonicated in acetone and methanol, dried under a flow of nitrogen and finally thermally heated until 900 ºC in oxygen flow. Polycrystalline substrates were cleaned in acetone and methanol and dried under a flow of nitrogen.

Concerning YBCO patterning, inkjet deposition was performed on 5x5 mm^2 LAO single crystal substrates. For LSMO patterning, deposition was done, first, onto 10x10 mm^2 LAO and STO single crystals and further on polycrystalline alumina, fused silica and Ni-metallic tapes.

High resolution photographs were registered through an Olympus BX51 microscope coupled to an Olympus DP20 camera.

Pattern dimensional characterization was performed by profilometric measurements using a profilometer Tenkor KLA.

X-ray Diffractometry (XRD) θ/2θ scans were carried out using a Siemens D500 diffractometer with Cu-K_α, λ=1.5418 Å.

Morphological analysis of the samples was studied by a scanning electron microscope SEM FEI Quanta 200 FEG.

YBCO tracks transport measurements were performed using a Physical Properties Measurement System (PPMS) from Quantum Design, in fields between 0 and 9 T and from 5 to 400 K.

Ink density was obtained by weighting in an analytical balance 1 mL of solution for three times.

Contact angle values were extracted from analysis of the images of 2 µL digitized sessile drops photographs. Surface tension data was obtained by evaluation of the video images of a pendant drop using a DSA100 equipment (KRÜSS, GmbH). The measurement procedure in both cases was an average of several independent measurements.

The viscosity of the YBCO precursor solution was evaluated by using a rheometer Haake RheoStress RS600 (Thermo Electro, GmbH) using a two parallel plate configuration and a gap of 200 µm which allows measuring the viscosity at high shear rates (86000 s^{-1}).

Results and discussion

Patterning of parallel YBCO tracks is particularly important in the development of HTS tapes with low ac losses. In that understanding, YBCO lines were successfully printed onto LAO single crystal substrate. By using a distance between drops of 20 µm and a line pitch of 400 µm it was possible to obtain independent YBCO tracks with a constant base width of about 150 µm. In **figures 1a and 1b,** it is shown optical micrographs of those tracks after pyrolysis process [9, 18]. In order to increase their thickness, four overprintings with an intermediate drying process at room temperature between depositions were performed. Moreover, as can be appreciated from figures 1a and 1b, continuous, straight and uniform YBCO tracks were achieved. Structural characterization by XRD after YBCO growth was carried out. From the XRD θ/2θ scan given in **figure 1c**, it can be observed that YBCO is single phase and c-axis aligned as expected from the low mismatch between the layer and the single crystal substrate. Further characterization based on two-dimensional XRD [19] (not shown here) have pointed out that YBCO film has grown over LAO single-crystal according to the epitaxial relation (001)YBCO[110]||(001)LAO[100]. Besides, YBCO tracks were morphologically characterized by SEM (**figure 1d to 1f**) displaying high homogeneity and uniformity along the whole track length.

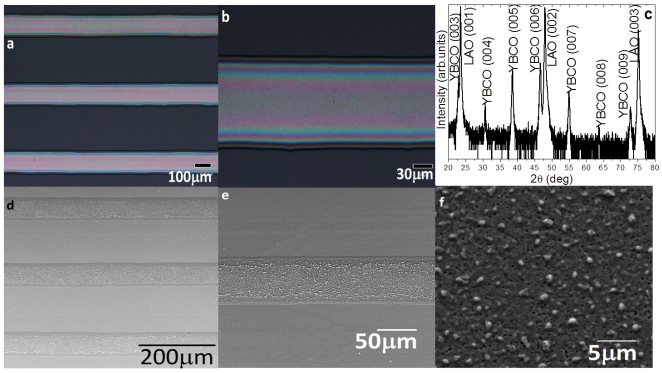

***Figure 1**. Morphological and structural characterization of YBCO printed tracks on LAO single crystal. (a) and (b) Optical microscopy images of precursor YBCO tracks printed after four overprintings. (c) XRD θ/2θ pattern of as-grown tracks. (d), (e) and (f) SEM micrographs after YBCO growth. In (d), (e) and (f) the sample plane was tilted 60 º downwards to obtain higher contrast.*

To determine the critical current density (J_c) of the sample, profilometric measurements were performed in order to determine the cross section profile. Cylinder sector shaped tracks, about 150 µm wide and 300 nm high, were obtained. The profile displayed for the tracks is absolutely coherent with surface tension of the ink and capillary forces (**figure 2a**). Critical current density (J_c) measurements were performed by the four probe standard transport method employing a 3 µV cm^{-1} electrical field criterion obtaining a maximum J_c at self field and 77K of 1.1 MA cm^{-2}. In **figure 2b**, it is presented the dependence of J_c with the magnetic field parallel to (00l) axis measured by injecting current along four tracks at the same time (Figure 2b red opened dot line) and along only two tracks at the same time (Figure 2b blue closed dot line). From figure 2b, it is clear that we have obtained two identical results measuring two sets of tracks suggesting so the homogeneity of its functional behavior.

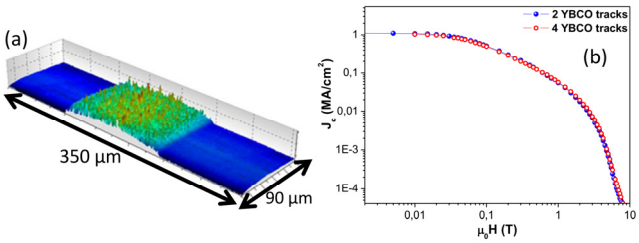

***Figure 2.** Profilometric and magnetic characterizations of as-grown YBCO tracks (a) 3D image of the surface of a YBCO track on LAO substrate. (b) Magnetic field dependence of the critical current density (J_c) measured for sets of two tracks (closed symbol) and four tracks (opened symbol) (see text for explanation).*

Regarding LSMO patterning, a circular LSMO full bridge was printed with four contact pads equidistributed around (**figure 3a**):

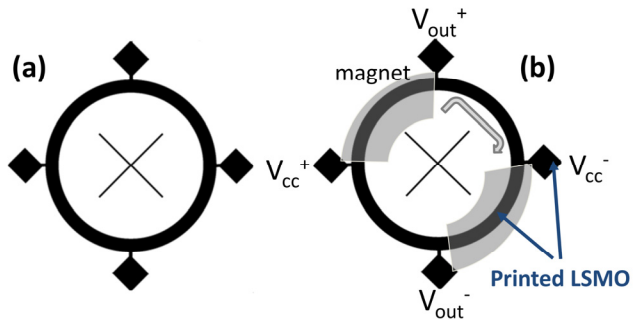

***Figure 3.** Conceptual detail of the rotational magnetoresistive LSMO contactless encoder. The design includes the circular bridge with its four contact pads for electrical connection (a) and the full sensor rig including the rotating magnet (b).*

According to **figure 3**, in the designed analog encoder, a magnetic assembly (grey parts in **figure 3b**) can rotate over the printed magnetoresistive bridge. It allows significant changes in the branch resistance. The bridge voltage output then varies according to the magnets position.

First trials were developed onto LAO and STO (10x10) mm^2 single crystals. It is worth to point out that high precision in the positioning of drops is necessary to avoid pattern irregularities and, therefore, to avoid large mismatch between the branches of the pattern. Given this fact, two strategies were attempted to increase surface energy and improve pattern resolution and accuracy. The first one was the printing of the LSMO device using the 2D interlacing technique and the second attempt was to pre-treat the

substrate surface with a polymer based solution enhancing the hydrophilic behaviour of the surface of the substrate.
By pre-treating the surface of the substrate with that polymeric solution, we could obtain a full bridge-like resistor system with resistances of about 10 KΩ per branch, including the contact pads. Morphological and magnetotransport characterizations were performed and reported below. **Figure 4a** depicts the whole (10x10) mm sample on a LAO single crystal substrate after LSMO growth. In **figure 4b** are shown SEM pictures where it is possible to observe the typical morphology of the granular manganite layer. It is worth to remark that the final layer shows to be epitaxial although the granular aspect of the surface obtained by the sinterization of the grains grown around the different seed nuclei. It is due to the epitaxial growth from the textured surface of the substrate. A minor polycrystalline fraction is occasionally observed although does not affect the magnetoresistance and resistivity of the material.

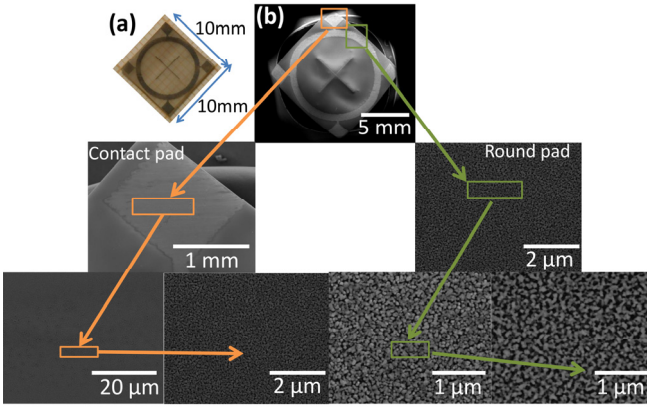

Figure 4. *Morphological characterization of the LSMO magnetoresistive device on a (10x10) mm LAO single crystal. (a) Optical micrograph of the general view of the magnetoresistive bridge. (b) SEM micrographs after LSMO growth of a contact and the round pad of the device.*

Magnetotransport measurements display magnetoresistance variations at 300K of about 0.5% at magnetic fields around 0.4T which can be well detected in a full bridge configuration.
Moreover, in order to evaluate the reproducibility of the inkjet printing process and to assess the suitability of the equipment, 20 LSMO devices on LAO and STO single crystals were printed (see **figure 5**). Each one consisted of four depositions and was printed by using the LSMO precursor ink of table 2.

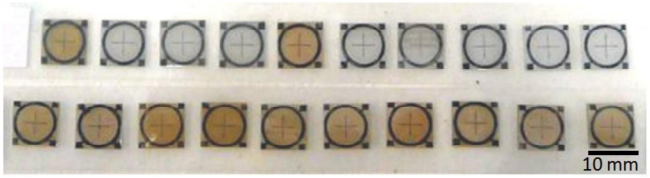

Figure 5. *Series of 20 LSMO full bridges printed over LAO (brown substrates) and STO (white substrates) single crystals displaying the feasibility of the inkjet printing technology.*

The promising results obtained for the LSMO device on single crystals encouraged us to devote effort towards decreasing the cost of the magnetoresistive devices. Due to electrical and magnetic properties of manganites are also observable in cheaper polycrystalline substrates, tests over polycrystalline alumina and fused silica (quartz glass) were also performed (**figure 6**).

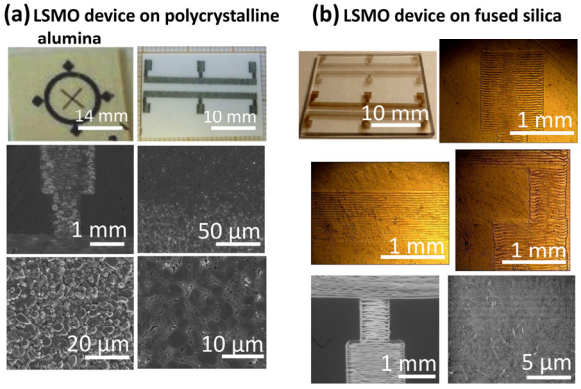

Figure 6. *LSMO devices on several polycrystalline non-textured substrates. Micrographs of several LSMO devices (a) over polycrystalline alumina. (b) over fused silica (quartz glass).*

The long length metallic substrates developed for CC's technology constitute a great opportunity to strongly reduce the cost of the LSMO devices. Getting profit about that substrate availability, preliminary investigations were developed over commercial epitaxial LZO coated ferromagnetic Ni RABIT tape (**figure 7**).

Figure 7. *Series of LSMO devices printed onto 10 mm Ni ferromagnetic metallic tape. An epitaxial LZO buffer layer is commercially available on top of this metallic substrate.*

In the case of polycrystalline alumina and fused silica substrates, resistance of the device in the range of 10-20 MΩ were measured. Beyond those results, and in order to decrease the branch's resistance, experiments increasing the number of drops per unit area are ongoing. However, previous experiments done with serigraphic pastes show that non-textured polycrystalline aggregates introduce a very high resistance through the grain boundaries. They affect the magnetoresistance and resistivity of the material revealing so the improvement achieved by inkjet printing driven CSD processing. Furthermore, additional optimization of the LSMO growth process on top of pre-coated metallic substrates is still required. Although the texturing ability of the commercial LZO buffer layer is proved, protection against metallic substrate oxidation should be improved. The high temperature of the thermal processing requires specific buffer layers able to stop oxygen diffusion. More research should be done in order to improve this promising option for this very low cost technique. Besides, parallel printheads were used successfully proving the high throughput capability of this methodology. Research is on the way.

Conclusions

Inkjet printing technology has demonstrated its huge flexibility and capacity for manufacturing of functional coatings based on the CSD approach. Specific devices could be performed at low manufacturing cost being possible counterpart of existing devices. In this communication, we show that it is possible to control the patterning of low ac losses superconducting coated conductors in only one production step. Also, more complex functional ceramic patterns have been demonstrated and tested. The high development level achieved by the metallic substrates for superconducting coated conductors has allowed their alternative use for manufacturing of electronic or magnetoelectronic devices with the added value of the possible contribution of the metallic substrate to the coating functionality (ferromagnetic behaviour) and the very low cost that could be achieved.

A door is open for a huge amount of applications and improvements.

Acknowledgments

The authors would like to acknowledge the financial support from EU (EFECTS 205854), MICCIN (CONSOLIDER NANOSELECT CSD2007-0041, MAT2011-28874-C02-01), Generalitat de Catalunya (Pla de Recerca 2009-SGR-770 and Xarmae) and CSIC (JAE).

References

[1] A. Llordés, A. Palau, J. Gázquez, M. Coll, R. Vlad, A. Pomar, J. Arbiol, R. Guzmán, S. Ye, V. Rouco, F. Sandiumenge, S. Ricart, T. Puig, M. Varela, D. Chateigner, J. Vanacken, J. Gutiérrez, V. Moshchalkov, G. Deutscher, C. Magen, and X. Obradors, "Nanoscale strain-induced pair supression as a vortex-pinning mechanism in high-temperature superconductors", Nature Mat. **11**, 329 (2012).

[2] T. M. Shaw, S. Trolier-McKinstry, and P. C. McIntyre, "The properties of ferroelectric films at small dimensions", Annu. Rev. Mater. Sci. **30**, 263 (2000).

[3] A. Hardy, D. Mondelaers, M. K. Van Vael, J. Mullens, L. C. Van Poucke, G. Vanhoyland, and J. D'Haen, "Synthesis of $(Bi,La)_4Ti_3O_{12}$ by a new aqueous solution gel-route", J. Eur. Ceram. Soc. **24**, 905 (2004).

[4] J. G. Wan, X. W. Wang, Y. J. Wu, M. Zeng, Y. Wang, H. Jiang, W. Q. Zhou, G. H. Wang, J. M. Liu, "Magnetoelectric $CoFe_2O_4$-$Pb(Zr,Ti)O_3$ composite thin films derived by a sol-gel process", Appl. Phys. Lett. **86**, 122501 (2005).

[5] M. Paranthanam, and T. Izumi, "High-performance YBCO-coated superconductor wires", Mat. Res. Bull. **8**, 533 (2004).

[6] Milton Ohring, Materials Science of thin films: deposition & structure (Academic Press, San Diego, CA, 2002) chapters 2,3,5,6,8

[7] A. B. Posadas, M. Lippmaa, F. J. Walker, M. Dawber, C. H. Ahn, and J. M. Triscone, "Growth and novel applications of epitaxial oxide thin films", Appl. Phys. **105**, 219 (2007).

[8] P. J. Hirst, and R. G. Humphreys, Handbook of Superconducting Materials (IoP ed, edited by D. A. Cardwell and D. S. Ginley, 2003) chapter B4.4.1, pg. 807.

[9] X. Obradors, T. Puig, A. Pomar, F. Sandiumenge, N. Mestres, M. Coll, A. Cavallaro, N. Romà, J. Gázquez, J.C. González, O. Castaño, J. Gutierrez, A. Palau, K. Zalamova, S. Morlens, A. Hassini, M. Gibert, S. Ricart, J.M. Moretó, S. Piñol, D. Isfort, and J. Bock, "Progress towards all-chemical superconducting YBCO coated-conductors", Supercond. Sci. Technol. **19**, s13 (2006).

[10] R. W. Schwartz, T. Schneller, and R. Waser, "Chemical solution deposition of electronic oxide films", C. R. Chimie. **7**, 433 (2004).

[11] H.Wijshoff, "The dynamics of the piezo inkjet printhead operation", Phys. Rep. **491**, 77 (2010).

[12] N. Amemiya, S. Kasai, K. Yoda, Z. Jiang, G. A. Levin, P. N. Barnes, and C. E. Oberly, "AC loss reduction of YBCO coated conductors by multifilamentary structure", Supercond. Sci. Technol. **17**, 1464 (2004).

[13] W. T. Norris, "Calculation of hysteresis losses in hard superconductors carrying ac: isolated conductors and edges of thin sheets", J. Phys. D: Appl. Phys. **3**, 489 (1970).

[14] S.R. Foltyn, L. Civale, J. L. Macmanus-Driscoll, Q. X. Jia, B. Maiorov, H. Wang, and M. Maley, "Materials science challenges for high-temperature superconducting wire", Nature, **6** (2007).

[15] A. Goyal, M. Paranthanam, and U. Schoop, " The RABITS approach: using rolling-assisted biaxially textured substrates for high-performance YBCO superconductors", Mat. Res. Bull. **8**, 552 (2004).

[16] I. Oijima, K. Kakimoto, Y. Yamada, T. Izumi, T. Saitoh, and Y. Shiohara, "Research and development of biaxially textured IBAD-GZO templates for coated conductors", Mat. Res. Bull. **8**, 564 (2004).

[17] A. Teichler, J. Perelaer, and U. S. Schubert, "Inkjet printing of organic electronics-comparison of deposition techniques and state-of-the-art developments", J. Mater. Chem. C, **1**, 1910 (2013).

[18] N. Roma, S. Morlens, S. Ricart, K. Zalamova, J. M. Moreto, A. Pomar, T. Puig, and X. Obradors, "Acid anhydrides: a simple route to highly pure organometallic solutions for superconducting films", Supercond. Sci. Technol. **19**, 521 (2006).

[19] B. B. He, Two dimensional X-ray diffraction (Wiley, 2009).